European Journal of Chemistry 8 (2) (2017) 168-173

European Journal of Chemistry

Journal webpage: www.eurjchem.com

Application of ethanol extracts of *Tapinanthus dodoneifolius* to inhibit annealed carbon corrosion in 2 M HCl and 3.5% NaCl solutions

Raphael Shadai Oguike *, Abdullahi Mohammad Shibdawa, Usman Ibrahim Tafida, Doris Ezekiel Amin Boryo and Florence Ikwo Omizegba

Corrosion Protection and Materials Science Laboratory, Department of Chemistry, Abubakar Tafawa Balewa University, PMB 0248 Bauchi, Nigeria

** Corresponding author at: Corrosion Protection and Materials Science Laboratory, Department of Chemistry, Abubakar Tafawa Balewa University, PMB 0248 Bauchi, Nigeria.*
Tel.: +234.903.3970383. Fax: +234.903.3970383. E-mail address: oguike.raphael@yahoo.com (R.S. Oguike).

ARTICLE INFORMATION

DOI: 10.5155/eurjchem.8.2.168-173.1558

Received: 23 February 2017
Received in revised form: 01 April 2017
Accepted: 05 April 2017
Published online: 30 June 2017
Printed: 30 June 2017

KEYWORDS

Adsorption
Annealed carbon
Biomass extracts
Elemental analysis
Corrosion inhibition
Tapinanthus dodoneifolius

ABSTRACT

Protection effect of ethanol extracts of *Tapinanthus dodoneifolius* leaf (TD extract) on corrosion of annealed carbon (FE164531) in 2 M HCl and 3.5% NaCl solution has been investigated by weight loss and electrochemical techniques. Surface morphology and elemental analysis was carried out on the corroded specimens using Scanning Electron Microscope/ Energy Dispersive X-ray Spectroscopy (SEM/EDS) to augment results obtained. The data obtained from weight loss revealed that the corrosion protection potentials of TD extract is temperature-concentration dependent. The effectiveness of protection against the corrosive environment increased with increasing TD extract concentration which decreased with increased temperature. Electrochemical polarization data showed TD extract suppressed both the cathodic and anodic processes on FE164531 specimen surface. Calculated thermodynamic parameters showed that TD extract adsorption process was spontaneous with likely electrostatic interactions which propose physical adsorption, a phenomenon consistent with unfavorable adsorption with increasing experimental temperature. The elemental analysis data show the presence of TD extract species on FE164531 surface supporting strong adsorption of extract constituents on the metal surface while SEM showed lesser corroded surface in the presence of TD extract.

Cite this: *Eur. J. Chem.* **2017**, *8(2)*, 168-173

1. Introduction

The low corrosion resistance of pure carbon steel is attributed to its incapacity to build up protective layer on the surface which controls the chemistry of the environment. Carbon steel which is the most cost effective engineering material can safely be operated in corrosive service conditions if corrosion control systems are properly designed and implemented. The use of inhibitors is widely accepted as paramount in cases of corrosion prevention. Moreover, some industrial divisions such as acid pickling, descaling processes, pipelines, chemical operation units, steam generators, oil and gas production units are all involved with inhibitors due to high corrosion rates in its process [1-4]. Due to increasing environmental awareness, researches on corrosion protection have moved attention to nontoxic inhibitors. Biomass extracts as metal corrosion inhibitors is beneficial in many respect and possess features for next generation corrosion inhibitors on the basis that they are inexpensive, readily available, nontoxic, and more especially, can provide a broad spectrum action based on the numerous molecular composition present in the aqueous extract among others [5]. Several authors have reported on the use of biomass extract to mitigate corrosion of carbon steel, mild steel, stainless steel, aluminum, magnesium and many other metal/alloys in both acid and alkaline solutions [6-11]. Numerous advantageous use of biomass extracts among others include that they are biodegradable, renewable and contain a number of organic compounds with similar electronic structures and functions that are comparable to conventional organic corrosion inhibitors.

Some authors believe that corrosion inhibitor efficiency basically point to their molecular structure [12-16] while the presence of unique atoms such as N, O and S in heterocyclic compounds has been widely reported to be an effective factor that enhances protection efficiency of inhibitors [17-20].

The current study presents the experimental assessment of the adsorption and corrosion inhibiting efficacy of ethanol extracts of *Tapinanthus dodoneifolius* leaves on annealed carbon in 2 M HCl and 3.5% NaCl solution corrosion. The experimental data were fitted into Langmuir adsorption isotherm while the effect of temperature gave thermodynamic parameters such as ΔH_{ads} and ΔS_{ads}. In addition to the experimental assessment, elemental analysis was done on the corroded surface to ascertain the presence of TD extract on the surface.

ISSN 2153-2249 (Print) / ISSN 2153-2257 (Online)
http://dx.doi.org/10.5155/eurjchem.8.2.168-173.1558

2. Experimental

2.1. Material preparation

Experiments were conducted using annealed carbon sheets of 99.5% purity obtained from Advent Research Materials (Eynsham, Oxford, England) with elemental composition (ppm) similar to the one presented elsewhere [21]. The annealed carbon sheet was press-cut into 4.0×4.0×0.1 cm dimensions as specimen with a hole of 1 mm drilled at the middle upper edge of specimen and were further abraded with metallographic emery paper of fineness pp1000. The specimens were prepared as described in our previous work [21] however, the extract was concentrated using rotatory evaporator. Inhibitor test solutions were prepared from the concentrate as described by Njoku *et al.*, [5] to get the desired concentrations. All test solutions were freshly prepared from analytical grade chemical reagent using bidistilled water while data analyses were carried out using Origin Pro8 Data analysis station and graphing workspace.

2.2. Weight loss

Previously cleaned FE164531 specimens were weighed to determine the initial weight thereafter, suspended under total immersion conditions in 250 mL beakers containing aerated and unstirred 200 mL test solutions, using glass hooks and rods. To determine the weight loss, the beakers were placed in a freely aerated thermostated water bath as reported by Oguike *et al.*, [21]. All tests were run in triplicate to verify the reproducibility of the results and the average data were reported. The weight loss experiment was realized using a B. BRAN digital weighing balance of the range 0.0001 to 160 g.

2.3. Electrochemical technique

The FE164531 specimens were further machined mechanically into dimensions of 1.5×1.5 cm^2 for the electrochemical experiments. Each specimen was appropriately sealed with thermosetting resin leaving exposed only 1.0 cm squared total surface area. The bare surface area was cautiously degreased using the procedure described for the weight loss experiment. Electrochemical test was conducted in a three-electrode corrosion cell as reported by reference [5]. Graphite rod and saturated calomel electrode (SCE) were used as counter and reference electrodes respectively while FE16451 was the working electrode. Measurements were performed in aerated and unstirred solutions at the end of 1 h immersion at open circuit potential (OCP) versus SCE. Potentiodynamic polarization scans were obtained within potential range of -0.25 mV to +1.6 mV *vs.* SCE and at a scan rate of 0.33 mV/s. Each experiment was run in triplicate to verify the reproducibility of the systems.

2.4. Surface characterization

The morphologies of the corroded FE164531 surfaces after 45 h of immersion were inspected on Vega Tescan scanning electron microscope, resolution 80 Angstroms, magnification range: 10× - 180000×, SE detector, HV 20.0 kV. FE164531 specimens were attached on top of an aluminum stopper by means of 3.0 M carbon conductive adhesive tape (SPI). The FE164531 specimens were coated with an ultra-thin coating of gold deposited on the surface using Quoirum Q150RS (Zeiss Systems, Germany) gold plating machine. This was done after the EDS spectra analysis. The Energy Dispersive X-Ray Emission Spectroscopy (EDS) were recorded in a VG TC INCA PentaFETx3 spectrometer with Mg K-X-ray source (1486.7 eV photons energy) operated at 300 W (accelerating voltage 12.5 kV, emission current 24 mA). The pressure in the analysis chamber did not exceed the value of 2.66×10^{-6} - 4.0×10^{-6} Pa during the entire period of spectra acquisition. All spectra were deconvoluted with EDS INCA software.

3. Results and discussions

3.1. Gravimetric results

The corrosion rate ($mm.y^{-1}$) for FE164531 specimens immersed in 2.0 M HCl and 3.5% NaCl solutions in the absence and presence of TD extract at varying temperatures are presented in Figure 1 while the protection exerted by different concentrations of TD extract as a function of temperature are shown in Figure 2. The result showed that TD extract appreciably retards the corrosion rate of FE164531 specimen in both 2.0 M HCl and 3.5% NaCl solutions indicating inhibition of the corrosion process. The protection efficiency (P%) of the extract was quantitatively evaluated by computing the ratio of corrosion rates in the presence of inhibitor (CR_2) with that in absence of the inhibitor (CR_1) as follows;

$$P\% = \left(1 - \frac{CR_2}{CR_1}\right) \times 100 \quad (1)$$

The results presented in Figure 2 show that protection efficiency increased with TD extract concentration but decreased with increased temperature. The protection efficiencies observed for TD extract in 2.0 M HCl and 3.5% NaCl solutions had their optimum at 1000 mg/L with temperature 303 K which indicates that the surface coverage of the substrate by the TD extract inhibitor attended an optimum level within low temperature.

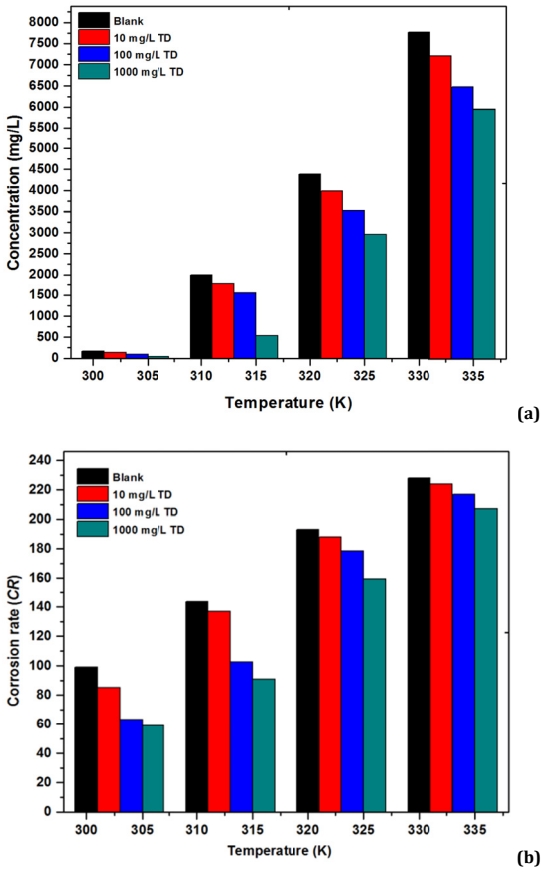

Figure 1. Corrosion rate ($mm.y^{-1}$) of FE164531 specimen as a function of TD leaf extract concentration and temperature determined by the weight loss (a) 2 M HCl solution (b) 3.5 % NaCl solution.

Table 1. Corrosion parameters obtained from potentiodynamic polarization scan for FE164531 in 2 M HCl solution in the absence and presence of TD leaf extract.

Solution	Parameters			
	i_{corr} (μA/cm²)	E_{corr} (mV(SCE))	θ	P_E %
Blank	5006.1	-357.28	-	-
10 mg/L	2409.18	-452.1	0.5188	51.88
100 mg/L	722.66	-453.9	0.8556	85.56
1000 mg/L	326.45	-467.8	0.9348	93.48

Table 2. Corrosion parameters obtained from potentiodynamic polarization scan for FE164531 in 3.5 % NaCl solution in the absence and presence of TD leaf extract.

Solution	Parameters			
	i_{corr} (μA/cm²)	E_{corr} (mV(SCE))	θ	P_E %
Blank	27.53	-695.72	-	-
100 mg/L	17.50	-710.35	0.3643	36.43
1000 mg/L	18.41	-680.68	0.3312	33.12

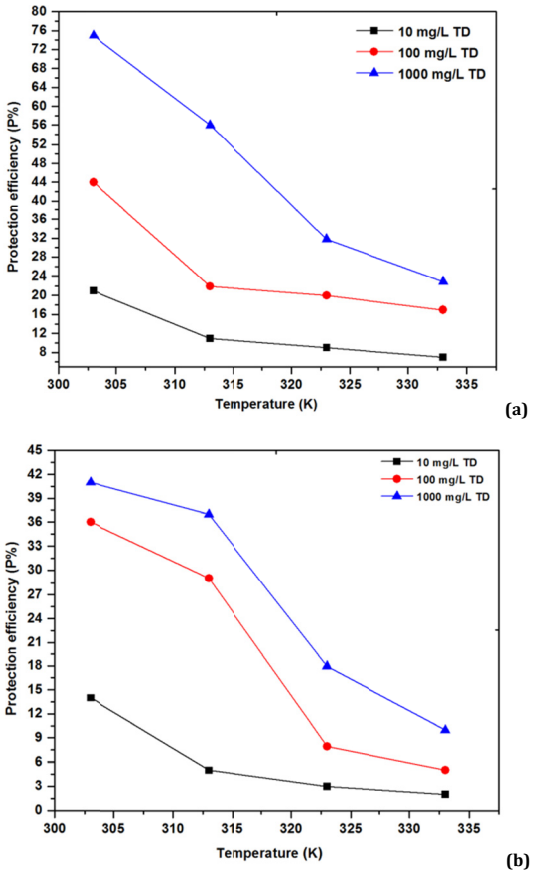

Figure 2. Protection efficiency (P%) of TD leaf extract on FE164531 specimen as a function of temperature (a) 2 M HCl solution (b) 3.5 % NaCl solution

3.2. Potentiodynamic polarization results

The potentiodynamic polarization plots help show the distinct effects of any inhibitor on the anodic and cathodic dissolution half reactions of various corrosion reactions. Representative polarization plots for the metal in 2.0 M HCl and 3.5% NaCl solutions in the absence and presence of different concentrations of TD extract are presented in Figure 3 and 4. The extracted polarization parameters obtained by extrapolation of Tafel slope are listed in Table 1 for FE164531 in 2.0 M HCl solution while Table 2 records the values for FE164531 in 3.5% NaCl solution, which were obtained by extrapolating the sequential division of the anodic and cathodic curves to the potential *x*-axis (Tafel extrapolation). It is clear from Figure 3, that TD extract decreased the current densities of both hydrogen gas evolution reactions ($2H^+ + 2e \rightarrow H_{2(g)}$) that is, cathodic corrosion process and the metal dissolution reaction ($Fe \rightarrow Fe^{2+} + 2e$) that is anodic corrosion process. This observed mitigation of both processes to some extent implies that TD extract functioned as a mixed-type inhibitor. However, except for the shift in the negative of E_{corr}, the polarization plots for all systems revealed that TD extract did alter the corrosion mechanism of the metal. The decrease in corrosion current density points to the fact that the inhibitor reduced material dissolution via adsorption on FE164531 surface. A different scenario was observed in 3.5% NaCl solution as seen in Figure 4. The introduction of TD extract did not shift the rest potential but a decrease in anodic current was noticed which further decreased with increasing concentration up to the optimum at 1000 mg/L. As observed (Table 2), TD extract had poor protection efficiency in 3.5% NaCl solution as recorded in the weight loss experiment and we decided to report results for 100 and 1000 mg/L of the extract. This poor protection efficiency is attributed to the action free Cl^- ions migrating through and undermining the adsorbed TD extract layer on the metal surface. From Table 1, it is also clear that addition of TD extract decreased the magnitude of the corrosion current density and as well slightly shifted E_{corr} towards more negative values. The value of corrosion current density in absence ($j_{corr\text{-}free}$) and presence ($j_{corr\text{-}inb}$) of different concentration of TD extract were used to quantify the magnitude of the protection efficiency (P_E%) using the Equation (2);

$$P_E\% = \left(1 - \frac{j_{corr-inh}}{j_{corr-free}}\right) \times 100 \qquad (2)$$

The results show higher P_E% value at higher TD extract concentration, in agreement with the gravimetric data.

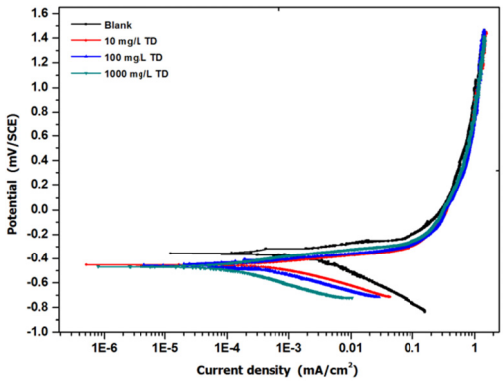

Figure 3. Potentiodynamic polarization curves for FE164531 specimen in aerated solution of 2 M HCl solution in the absence and presence of TD extract.

Table 3. Thermodynamic activation parameters of TD leaf extract adsorption on FE164531 specimens.

Sample	2 M HCl			3.5 % NaCl		
	ΔS^*_{ads} (×10^{18}) J/mol.K	ΔH^*_{ads} (×10^{21}) J/mol	r^2	ΔS^*_{ads} (×10^{19}) J/mol.K	ΔH^*_{ads} (×10^{20}) J/mol	r^2
Blank	-3.41	2.85	0.8399	-1.11	5.87	0.9639
10 mg/L	-3.05	2.97	0.8382	-1.09	6.72	0.9603
100 mg/L	-2.54	3.15	0.8242	-1.05	8.03	0.9788
1000 mg/L	-0.44	3.85	0.9277	-0.97	10.49	0.9902

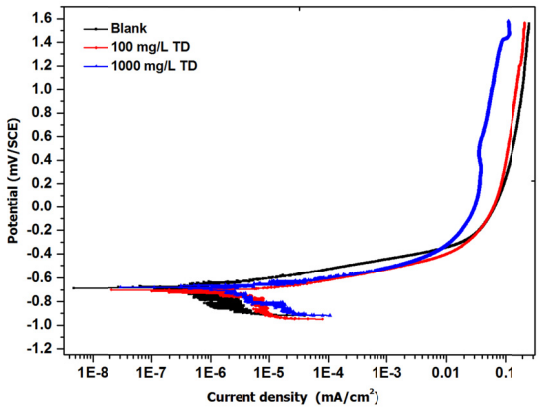

Figure 4. Potentiodynamic polarization curves for FE164531 specimen in aerated solution of 3.5% NaCl solution in the absence and presence of TD extract.

3.3. Thermodynamic consideration

Thermodynamic functions for dissolution of FE164531 in 2 M HCl and 3.5% NaCl solution in the absence and presence of TD extract were obtained by applying the transition state equation below;

$$CR = \left(\frac{R.T}{N.h}\right) \exp\left(\frac{\Delta S^*_{ads}}{R}\right) \exp\left(\frac{\Delta H^*_{ads}}{R.T}\right) \quad (3)$$

where, CR is the corrosion rate, N is Avogadro's number, h is plank's constant, T is absolute temperature and R is universal gas constant.

Transition state linear plots of TD extract action shown in Figure 5 has a slope of ($-\Delta H^*/2.303 \cdot R$) and intercept of [Log($R$/N.$h$) + ($\Delta S$/2.303.$R$)] from which the values of ΔH^* and ΔS^* were evaluated. Obtained data indicates that TD extract had high activation enthalpy and entropy values with the entropy values being higher in 3.5% NaCl solution which produced more disorderliness and lower protection efficiency. Table 3 shows the values acquired from the transition state plot for enthalpy of activation and entropy of activation for the dissolution and inhibition of FE164531 in both solutions. The positive sign of ΔH^* shows the endothermic nature of the process suggesting increase in temperature increases dissolution and retards protection efficiency. The entropy of activation (ΔS^*) values were negative indicating a spontaneous process of dissolution and the presence of TD extract induced an orderly fashion as the values were seen to decrease negatively via adsorption occurring at the metal surface.

3.4. SEM/EDS analysis results

The obtained micrographs of representative areas of corroded FE145631 surface after 45 hours of immersion in 2 M HCl and 3.5% NaCl solution in absence and presence of TD extract are shown in Figure 6 and 7. The surface examination revealed that the FE145631 specimen was severely corroded in 2 M HCl solution revealing rough and nodular surface with shallow pits distributed over the surface while in 3.5% NaCl solution, the surface was corroded with high density spherical pits all over. The observed precipitates on the metal surface (Figure 6b) might be NaCl crystals that were not washed out during rinsing after the immersion test. The corrosion prone FE145631 surface confirms the unstable state of FeO which actually oxidizes to soluble Fe_2O_3 and Fe_3O_4 via the equation below:

$$3FeO + O^{2-} \rightarrow Fe_3O_4 + 2e \quad (4)$$

$$2Fe_3O_4 + O^{2-} \rightarrow 3Fe_2O_3 + 2e \quad (5)$$

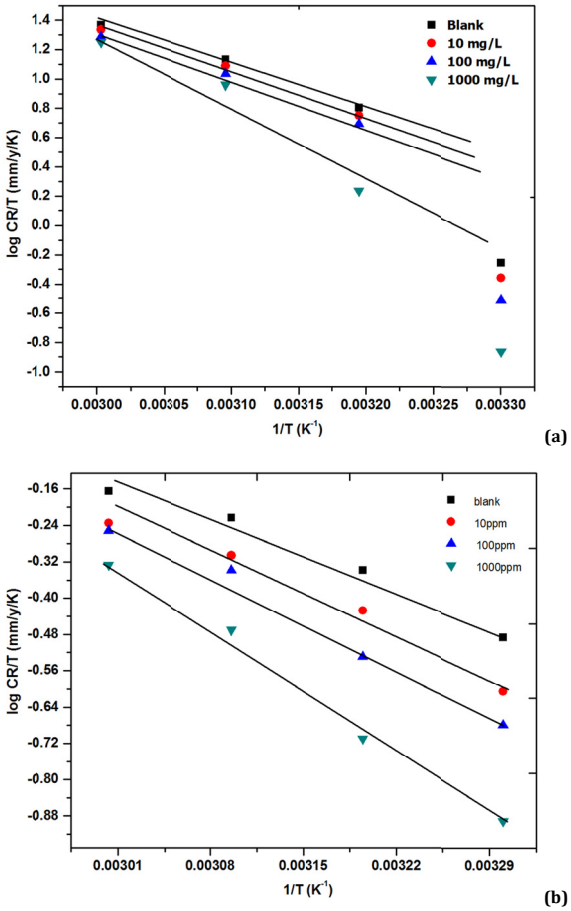

Figure 5. Transition state theory plot of TD extracts on FE164531 specimen in (a) 2 M HCl, (b) 3.5% NaCl solution.

Fe_3O_4 is known to form protective film on Fe surface that is not compact and quickly oxidize to Fe_2O_3 that is porous and leaf Fe surface into the bulk solution enhancing dissolution of the protective film (if any). TD extract is seen to have protected the surface to a good degree due to complex chelating ligands formed with Fe atoms. As expected, due to the electron affinity Fe atoms has for nitrogen and sulphur atoms, TD extract molecular composition might directly adsorb on a molecular plane parallel to FE145631 surface to form S-Metal-N chelate ligands as confirmed by the EDS analysis spectra. This is in concession with the findings of Kosari *et al.* [22].

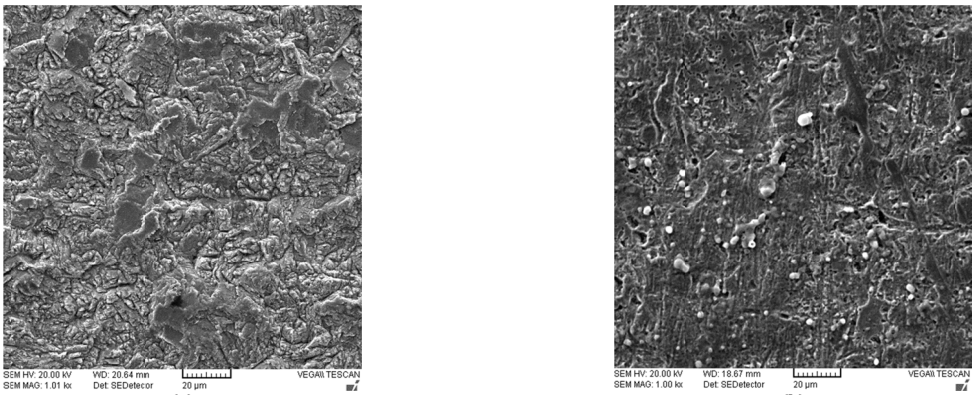

Figure 6. SEM micrographs of FE145631 surface after immersion for 45 h in (a) 2 M HCl (b) 3.5% NaCl solutions without inhibitor.

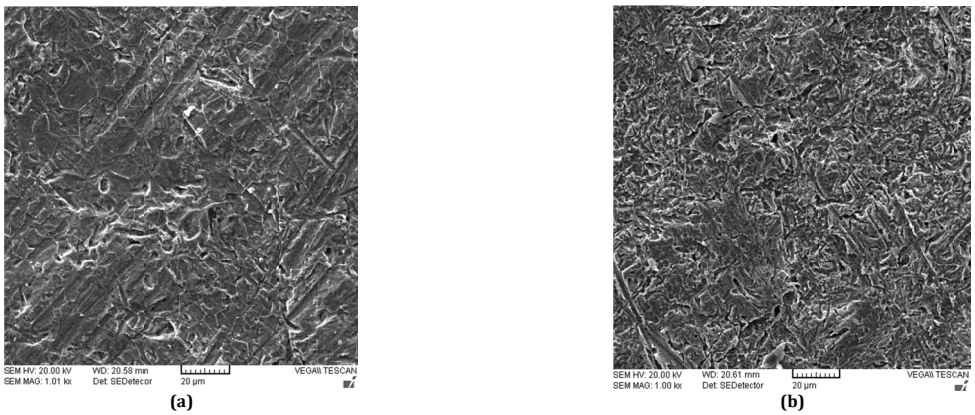

Figure 7. SEM micrographs of FE145631 surface after immersion for 45 h in (a) 2 M HCl (b) 3.5% NaCl solutions with TD extract as inhibitor.

The corroded FE145631 in 3.5% NaCl solution showed straight groves on the surface as a result of corrosion along mechanical faults caused during mechanical polishing of the metal surface. TD extract is seen to adsorb along these mechanical faults as they were barely visible (Figure 6), an indication that TD extract could sufficiently protect Fe surface in various media effectively.

3.5. Elemental analysis

Energy dispersive X-ray analysis gave additional information about the protection mechanism of the extract constituents. It is widely accepted that the process of inhibiting corrosion is associated with formation and growth of insoluble stable film on metal surface through the process of complexation of the inhibitor molecules [22]. EDS analysis of the corroded specimen surfaces after immersion test was performed to characterize any surface film and corrosion deposits formed. The results obtained are as shown in Figure 8-11. The results for 2 M HCl solution with the inhibitor extract presented in Figure 9 reveals high oxygen peak signal suggesting that the main corrosion product of carbon steel in HCl is a non-stoichiometric Fe^{3+} oxide/oxyhydroxide, consisting of a mixture of FeO(OH) and Fe_2O_3, where FeO(OH) is the main phase as reported by Samide *et al*. [23]. The high peak for carbon atoms appeared in the inhibited specimen suggest an interaction of carbon molecules with the specimen surface via electrostatic interaction, moreover, the high strength of peak could be from the carbon tape (SPI) used for the specimen stub. The presence of oxygen as well as minor amount of sulphur, nitrogen and chlorine disclosed by EDS analysis indicates the presence of iron oxide and complexing ligands of S and N on the specimen surface. The EDS spectra confirmed that the corrosion products that formed on FE145631 was FeO, possibly with traces of (N-Fe-S)ads and (Fe-Cl-TD)ads. This agrees with the view of El-Sayed [24] that inhibition process involves the formation of chelate on the metal surface via electron exchange that leads to coordinate covalent bond. The EDS spectra for Fe in 3.5% NaCl solution included phosphorrous and potassium atoms indicating more adsorption sites on FE surface. The presence of silicon and sodium atoms is suspected to be due to the precipitates from the NaCl solution.

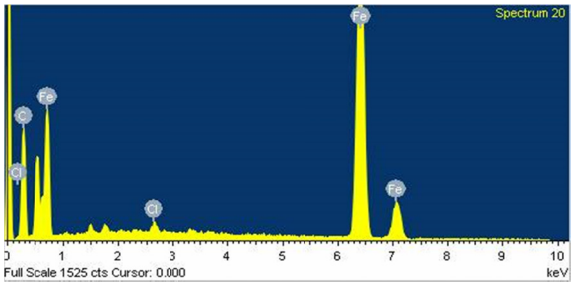

Element	Weight %	Atomic %
C	32.79	69.29
Cl	0.63	0.45
Fe	66.58	30.26
Totals	100.00	100.00

Figure 8. EDS analysis of the corrosion products on FE145631 surface in 2 M HCl solution without inhibitor.

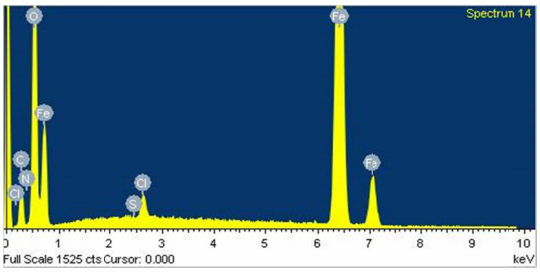

Element	Weight %	Atomic %
C	9.45	22.57
N	0.68	1.39
O	23.10	41.40
S	0.10	0.09
Cl	1.06	0.86
Fe	65.61	33.69
Totals	100.00	100.00

Figure 9. EDS analysis of the corrosion products on FE145631 surface in 2 M HCl solution in the presence of TD extract.

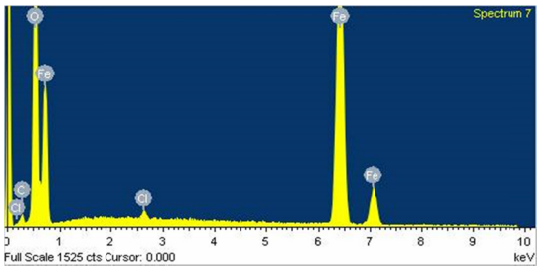

Element	Weight %	Atomic %
C	3.35	8.32
O	29.94	55.86
Cl	0.53	0.45
Fe	66.19	35.37
Totals	100.00	100.00

Figure 10. EDS analysis of the corrosion products on FE145631 surface in 3.5% NaCl solution without inhibitor.

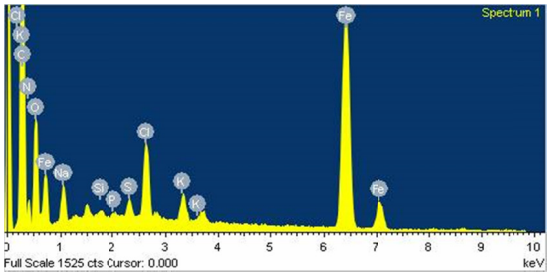

Element	Weight %	Atomic %
C	49.30	65.52
N	10.77	12.28
O	13.65	13.62
Na	1.22	0.85
Si	0.10	0.06
P	0.10	0.05
S	0.39	0.20
Cl	2.05	0.92
K	0.78	0.32
Fe	21.63	6.18
Totals	100.00	100.00

Figure 11. EDS analysis of the corrosion products on FE145631 surface in 3.5% NaCl solution in the presence of TD extract.

4. Conclusions

The objective of this study was to assess TD leaf extract for corrosion protection ability on annealed iron (FE145631) in 2 M HCl and 3.5% NaCl solution and to attempt explaining the protection process. Our results did show that corrosion protection was achieved via the organic species from the leaf extract found on the Fe surface as a result of adsorption. One of the interesting conclusions from this study is that the adsorbed organic species modified the nature of the passivation potential the metal exhibited in both media which remarkably improved positively the adsoprtion activation enthalpy. We have also used SEM/EDS to characterize the extent of protection and possible corrosion products on Fe surface. The results showed reasonable peaks for N, O and S attributed to spontaneous adsorption of the leaf's constituents on the Fe surface, hence credited responsible for the observed corrosion inhibiting efficacy of TD leaf extract.

Acknowledgements

The authors are grateful to Goddy Oguike (Deloitte, UK) for sponsoring the publication of this paper and also Tertiary Education Trust Fund Nigeria 2015/2016 intervention for sponsoring part of the laboratory works. Professor Alan Hodgson, Director of Electron Microscope Unit, Rhodes University, Grahamstown, South Africa and Professor Emeka Oguzie, Director of Centre for Research, innovation and Development, Federal University of Technology Owerri, Nigeria are also appreciated for making available the equipment for surface morphology and electrochemical analysis, respectively.

References

[1]. Ozcan, M.; Karadag, F.; Dehri, I. *Acta Phys. Chim. Sin.* **2008**, *24*, 1387-1392.
[2]. El-Etre, A. Y.; Abdallah, M.; El-Tantawy, Z. E. *Corros. Sci.* **2005**, *47*, 385-395.
[3]. Oguike, R. S. *Adv. Mater. Phys. Chem.* **2014**, *4*, 153-163.
[4]. Arukalam, I. O.; Madufor, I. C.; Ogbobe, O.; Oguzie, E. E. *Brit. J. Appl. Sci. Tech.* **2014**, *4*, 1445-1460.
[5]. Njoku, D. I.; Ukaga, I.; Ikenna, O. B.; Oguzie, E. E.; Oguzie, K. L.; Ibisi, N. *J. Mol. Liq.* **2016**, *219*, 417-424.
[6]. Zhang, Y. N.; Zi, J. L.; Zheng, M. S.; Zhu, J. W. *J. Alloy Compd.* **2008**, *462*, 240-243.
[7]. Deyab, M. A.; Eddahaoui, K.; Essehli, R.; Rhadfi, T.; Benmokhtar, S.; Mele, G. *Desalination* **2016**, *383*, 38-45.
[8]. Ekpe, U. J.; Okafor, P. C.; Ebenso, E. E.; Offiong, O. E.; Ita, B. I. *Bul. Electrochem.* **2001**, *17*, 131-135.
[9]. Khaled, K. F. *Corros. Sci.* **2010**, *52*, 3225-3234.
[10]. El-Etre, A. Y.; Abdallah, M.; El-Tantawy, Z. E. *Corros. Sci.* **2005**, *47*, 385-395.
[11]. Lopez, D. A.; Simison, S. N.; Sanchez, S. R. *Electrochim. Acta* **2003**, *48*, 845-854.
[12]. Rodriguez-Valdez, L. M.; Martinez-Villafane, A.; Glossman-Mitnik, D.; Ju, H.; Zhao, P.; Liang, Q.; Li, Y. *Appl. Surf. Sci.* **2005**, *252*, 1596-1607.
[13]. Lesar, A.; Milosev, I. *Chem. Phys. Lett.* **2009**, *483*, 198-203.
[14]. Bentiss, F.; Mernari, B.; Traisnel, M.; Vezin, H.; Lagrenee, M. *Corros. Sci*. **2010**, *53*, 487-495.
[15]. Kai, Z. P.; Li, Y. *Corros. Sci*. **2008**, *50*, 865-871.
[16]. Oguzie, E. E.; Wang, S. G.; Li, Y.; Wang, F. H. *J. Phys. Chem. C* **2009**, *113*, 8420-8429.
[17]. John, S.; Joseph, B.; Balakrishnan, K. V.; Aravindakshan, K. K.; Joseph, A. *Mater. Chem. Phys.* **2010**, *123*, 218-224.
[18]. Oguike, R. S.; Kolo, A. M.; Shibdawa, A. M.; Gyenna, H. A. *ISRN Phys. Chem.* **2013**, 175910, 1-9.
[19]. Raja, P. B.; Sethuraman, M. G. *Mater. Lett.* **2008**, *62*, 113-116.
[20]. Lebrini, M.; Traisnel, M.; Lagrenee, M.; Mernari, B.; Bentiss, F. *Corros. Sci*. **2008**, *50*, 473-479.
[21]. Oguike, R. S.; Kolo, A. M.; Ayuk, A. A.; Eze, F. C.; Oguzie, E. E. *Am. Chem. Sci. J.* **2015**, *8*, 1-12.
[22]. Kosari, A.; Moayed, M. H.; Davoodi, A.; Parvizi, R.; Momeni, M.; Eshghi, H.; Moradi, H. *Corros. Sci.* **2014**, *78*, 138-150.
[23]. Samide, A.; Tutunaru, B.; Negrila, C. *Chem. Biochem. Eng. Q.* **2011**, *25*, 299-308.
[24]. El-Sayed, N. H. *Eur. J. Chem.* **2016**, *7(1)*, 14-18.